Synthesis of Tetrametallic Thiolate-bridged Fe_3Au Clusters. Crystal Structure of $[Fe_3(CO)_9(\mu_3\text{-}SPr^i)\{\mu\text{-}Au(PPh_3)\}]$ †

Esther Delgado,*[,a] **Elisa Hernández,**[a] **Oriol Rossell,**[b] **Miquel Seco**[b] **and Xavier Solans**[c]
[a] *Departamento de Química Inorgánica, Facultad de Ciencias, Universidad Autónoma de Madrid, 28049 Madrid, Spain*
[b] *Departament de Química Inorgànica, Facultat de Química, Diagonal 647, 08028 Barcelona, Spain*
[c] *Departament de Cristal.lografia, Mineralogia i Dipòsits Minerals, Universitat de Barcelona, Martí i Franqués s/n-08028 Barcelona, Spain*

The reaction of the lithium salt of $[Fe_3(CO)_9(\mu_3\text{-}SR)]^-$ with $[Au(PPh_3)Cl]$, in the presence of $TlBF_4$, gives high yields of the new tetrametallic clusters $[Fe_3(CO)_9(\mu_3\text{-}SR)\{\mu\text{-}Au(PPh_3)\}]$ (R = Pr^i **1**, Bu^t **2**, C_6H_{11} **3** or Et **4**). Clusters **3** and **4** were formed along with the dimetallic species $[Fe_2(CO)_6(\mu\text{-}CO)(\mu\text{-}SR)\{\mu\text{-}Au(PPh_3)\}]$ (R = C_6H_{11} **5** or Et **6**). The structure of **1** has been determined by X-ray diffraction methods. The metal core consists of an isosceles triangle of iron atoms, capped by a SPr^i ligand and the longest iron–iron bond is bridged by an $Au(PPh_3)$ fragment. The fast atom bombardment mass spectra of the positive ions of **1**–**4** show a similar pattern to that reported for $[Fe_3(CO)_9(\mu_3\text{-}SR)(\mu\text{-}H)]$ consisting of a primary fragmentation involving stepwise loss of carbonyl groups from the parent ion to give $[Fe_3(SR)\{Au(PPh_3)\}]^+$, followed by elimination of an olefinic group to give $[Fe_3(SH)\{Au(PPh_3)\}]^+$ and finally loss of hydrogen to afford $[Fe_3(S)\{Au(PPh_3)\}]^+$.

Iron–gold clusters containing one or more $Au(PR_3)$ fragments are very common and reveal the great interest in the field of heteronuclear transition-metal clusters as a whole.[1] In most cases, the gold moiety can adopt either edge-bridging or face-capping bonding modes[2] because of its a_1 hybrid (*s*–*z*). However, some examples of complexes in which the iron–gold interaction can be understood on the basis of a two-centre two-electron bonding interaction have recently been reported and structurally characterized and include two unusual tetrametallic Fe_2Au_2 clusters.[3,4] In addition, in several iron–gold complexes, the iron–iron bonds appear to be bridged by ligands such as sulfur,[5] phosphido,[6] substituted ethenyl,[7] COMe[8] or $HC{=}NBu^t$,[9] which enhance the thermodynamic stability of the resulting product. Recently, we have described the synthesis of a series of iron–gold clusters containing thiolate bridging ligands of formula $[Fe_2(CO)_6(\mu\text{-}CO)(\mu\text{-}SR)\{\mu\text{-}Au(PPh_3)\}]$ (R = Pr^i, Bu^t or Ph) in an effort to correlate the stability of these species with the stereochemistry of the R group of the thiol.[10] With the aim of extending these studies to metal clusters of higher nuclearity, we have begun a study involving the trimetallic thiolate-bridged $[Fe_3(CO)_9(\mu_3\text{-}SR)]^-$ anions which are used as building blocks for the synthesis of neutral tetrametallic $[Fe_3(CO)_9(\mu_3\text{-}SR)\{\mu\text{-}Au(PPh_3)\}]$ derivatives. We were mainly interested in determining the bonding mode adopted by the $Au(PPh_3)$ group in such complexes and in comparing their most interesting structural features with the related trimetallic Fe_2Au clusters.

Results and Discussion

It is well established that the reaction of thiols, RSH, with $[Fe_3(CO)_{12}]$ produces trinuclear $[Fe_3(CO)_9(\mu_3\text{-}SR)(\mu\text{-}H)]$ derivatives[11] through the rupture of the S–H bond. Given the isolobal analogy between the H^+ and the $Au(PPh_3)^+$ fragments,[12] our first attempts to synthesize the Fe_3Au clusters involved the use of the recently described thiolate gold complexes, $[Au(PPh_3)(SR)]$ (R = Pr^i, Bu^t, Et or C_6F_5).[13] These were allowed to react with the trinuclear iron carbonyl complex, $[Fe_3(CO)_{12}]$, but in no case were mixed iron–gold complexes formed and mixtures of the dinuclear species $[Fe_2(CO)_4(PPh_3)_2(\mu\text{-}SR)_2]$ and $[Fe_2(CO)_5(PPh_3)(\mu\text{-}SR)_2]$ were obtained instead. As a result we decided to try another synthetic method involving the following steps: (*i*) preparation of the iron anion $[Fe_3(CO)_9(\mu_3\text{-}SR)]^-$ by reaction of the salt LiSR, prepared from RSH and LiBu in tetrahydrofuran (thf) at −78 °C, with $[Fe_3(CO)_{12}]$ at 40 °C and (*ii*) reaction of the lithium salt of the anion $[Fe_3(CO)_9(\mu_3\text{-}SR)]^-$ with $[Au(PPh_3)Cl]$ in the presence of $TlBF_4$ as a halide abstractor in thf at room temperature, according to equation (1).

$$[Fe_3(CO)_9(\mu_3\text{-}SR)]^- + [Au(PPh_3)Cl] + TlBF_4 \longrightarrow [Fe_3(CO)_9(\mu_3\text{-}SR)\{\mu\text{-}Au(PPh_3)\}] + TlCl + LiBF_4 \quad (1)$$

	R
1	Pr^i
2	Bu^t
3	C_6H_{11}
4	Et

In the first step, along with the iron anion $[Fe_3(CO)_9(\mu_3\text{-}SR)]^-$, the dinuclear $[\{Fe(CO)_3(\mu\text{-}SR)\}_2]$ is also formed as a by-product, but it can easily be separated by extraction with hexane, after solvent evaporation. The synthesis of the iron anion reported here is an improvement of the method previously described by Takács and Markó[14] since it does not require high temperatures thus affording better yields. However, it should be noted that the scope of this process is limited to thiols containing R groups such as Bu^t, Pr^i, C_6H_{11} or Et. For R = Ph, CH_2Ph or C_6F_5 the formation of the iron anion was not detected and only $[\{Fe(CO)_3(\mu\text{-}SR)\}_2]$ was identified by IR spectroscopy as the main product. This surprising behaviour does not agree with those reports[11] indicating that only

---

† *Supplementary data available:* see Instructions for Authors, *J. Chem. Soc., Dalton Trans.*, 1993, Issue 1, pp. xxiii–xxviii.

Table 1 Analytical data and physical parameters of complexes **1–6**

Compound	Analysis^a (%)			NMR		
	C	H	ν(CO)^b/cm^{-1}	δ(^{31}P)^c	δ(^{1}H)^d	δ(^{13}C)^{d,e}
1	38.75 (37.80)	2.35 (2.30)	2050m, 2004vs, 1996(sh), 1973s, 1952m, 1934w	54.8^b	1.65 (d, 6 H, CH_3, J = 6, 3), 4.16 (m, 1 H, CH), 7.45 (m, 15 H, PPh_3)	212.9 (s, 9 CO), 133.9–129.0 (PPh_3), 48.7 (s, 1 C, CH), 24.5 (s, 2 C, CH_3)
2	38.35 (38.45)	2.60 (2.50)	2049m, 2003vs, 1995(sh), 1971s, 1947m, 1934w	54.6^b	1.72 (s, 9 H, CH_3), 7.50 (m, 15 H, PPh_3)	213.2 (s, 9 CO), 133.9–129.0 (PPh_3), 63.3 (s, 1 C, SC), 31.9 (s, 3 C, CH_3)
3	41.25 (39.85)	2.95 (2.60)	2049m, 2004vs, 1995(sh), 1971s, 1950m, 1934w	54.8^b	2.28 (m, 1 H, CH), 1.21–1.63 (m, 10 H, C_6H_{11}), 7.46 (m, 15 H, PPh_3)	213.1 (s, 9 CO), 133.9–129.2 (PPh_3), 68.2 (s, 1 C, CH), 35.6 (s, 2 C, CH_2^{f}), 26.6 (s, 1 C, CH_2^{g}), 25.0 (s, 2 C, CH_2^{h})
4	37.85 (37.05)	2.15 (2.15)	2049m, 2004vs, 1997(sh), 1970s, 1946m, 1919w	59.0^e	1.70 (t, 3 H, CH_3, J = 7.5), 3.89 (q, 2 H, CH_2, J = 7.4), 7.49 (m, 15 H, PPh_3)	212.7 (s, 9 CO), 133.6–128.8 (PPh_3), 38.5 (s, 1 C, CH_2), 16.2 (s, 1 C, CH_3)
5	42.70 (42.20)	3.20 (2.95)	2049m, 2016vs, 1971s, 1784m	57.1^e	0.75–2.1 (m, 11 H, C_6H_{11}), 7.48 (m, 15 H, PPh_3)	218.0, 211.8, 209.7 (6 CO), 133.7–128.4 (PPh_3), 67.8 (s, 1 C, CH), 37.1 (s, 2 C, CH_2^{f}), 25.5 (s, 2 C, CH_2^{g}), 25.3 (s, 2 C, CH_2^{h})
6	40.30 (39.15)	2.30 (2.40)	2048m, 2016vs, 1974s, 1783m	57.3^e	1.28 (t, 3 H, CH_3), 2.34 (q, 2 H, CH_2), 7.43 (m, 15 H, PPh_3)	215.6, 210.9, 208.0 (6 CO), 135.0–129.0 (PPh_3), 37.6 (s, 1 C, CH_2), 18.0 (s, 1 C, CH_3)

[a] Required values are given in parentheses. [b] In thf. [c] Referenced to H_3PO_4. [d] Referenced to $SiMe_4$. [e] In $CDCl_3$. [f] *ortho*-C. [g] *meta*-C. [h] *para*-C.

secondary and tertiary thiols can react with $[Fe_3(CO)_{12}]$ to give the hydride–iron complexes $[Fe_3(CO)_9(\mu_3\text{-SR})(\mu\text{-H})]$. At this point, neither electronic nor steric factors can clearly explain the different behaviour of thiols or lithium thiolates when treated with triiron carbonyls and further effort is thus needed in this area.

The second step involving the synthesis of mixed iron–gold clusters from a carbonylmetalate and a metal halide complex is one of the best known methods to obtain mixed-metal cluster compounds containing one or more Group 11 metals.[2] Generally, it appears to be a clean, high-yield route. However, in this case, the formation of the red iron–gold clusters $[Fe_3(CO)_9(\mu_3\text{-SR})\{\mu\text{-Au}(PPh_3)\}]$ is accompanied by other undesirable by-products. Thus, for R = C_6H_{11} or Et, we have isolated, after chromatographic work-up, the orange dimer $[\{Fe(CO)_3(\mu\text{-SR})\}_2]$ in low yield, traces of the starting anion, and, more interestingly, green $[Fe_2(CO)_6(\mu\text{-CO})(\mu\text{-SR})\{\mu\text{-Au}(PPh_3)\}]$ clusters. The latter derivatives can be considered to have been formed by loss of an $Fe(CO)_3$ group from the tetrametallic complexes. The tendency of the starting $[Fe_3(CO)_9(\mu_3\text{-SR})]^-$ anion to cleave one Fe–Fe bond had been noted previously in its reaction with the monohalides XCl [X = PR_2, AsR_2, *etc.* (R = alkyl)] to yield $[Fe_3(CO)_9(\mu_3\text{-SR})(\mu\text{-X})]$.[15] This is the first report of the compound $[Fe_2(CO)_6(\mu\text{-CO})(\mu\text{-SC}_6H_{11})\{\mu\text{-Au}(PPh_3)\}]$ **5** and, again surprisingly, by this route we were able to obtain the trimetallic $[Fe_2(CO)_6(\mu\text{-CO})(\mu\text{-SEt})\{\mu\text{-Au}(PPh_3)\}]$ **6** in moderate to high yields (60%). We had been unable to synthesize this compound by treating $[Fe_2(CO)_6(\mu\text{-CO})(\mu\text{-SEt})]^-$ with $[Au(PPh_3)Cl]$.[10] The unexpected formation of **6** contradicts our initial explanation that the initial failure in its isolation was due to its extremely high instability.

The new complexes have been characterized by elemental analysis and IR, ^{1}H, ^{31}P and ^{13}C NMR spectroscopy (Table 1) as well as by fast-atom bombardment (FAB) mass spectrometry (Table 2). The solution infrared spectra of **1–4** are almost identical and contain no peak in the bridging carbonyl stretching region, as observed for the related $[Fe_3(CO)_9(\mu_3\text{-SR})(\mu\text{-H})]$.[16] Furthermore the ν(CO) bands are shifted to slightly higher frequencies with respect to the corresponding iron anions[17] indicating a decrease in electron density in the iron atoms. Proton and ^{13}C NMR spectra reveal the presence of the organic and carbonyl groups whereas the ^{31}P NMR spectra of their thf solutions consist of one signal due to the $Au(PPh_3)$ ligand.

Table 2 FAB mass spectra of compounds **1–6**

Compound	m/z
1	954 (M^+), 898, 870, 842, 814, 786 (M^+ − nCO, n = 2–6), 730 (M^+ − 8 CO), 702 (M^+ − 9 CO), 660 $[Fe_3\{Au(PPh_3)\}(SH)]$, 659 $[Fe_3\{Au(PPh_3)\}S]$, 459 $[Au(PPh_3)]$, 721 $[Au(PPh_3)_2]$, 994 $[Au_2(SPr^i)(PPh_3)_2]$
2	968 (M^+), 912, 884, 856, 828, 800, 772, 744, 716 (M^+ − nCO, n = 2–9), 660 $[Fe_3\{Au(PPh_3)\}(SH)]$, 659 $[Fe_3\{Au(PPh_3\}S]$, 459 $[Au(PPh_3)]$, 721 $[Au(PPh_3)_2]$, 1007 $[Au_2(SBu^t)(PPh_3)_2]$
3	994 (M^+), 966, 938, 910, 882, 854, 826, 798, 770, 742 (M^+ − nCO, n = 1–9), 660 $[Fe_3\{Au(PPh_3)\}(SH)]$, 659 $[Fe_3\{Au(PPh_3)\}S]$, 459 $[Au(PPh_3)]$, 721 $[Au(PPh_3)_2]$, 1033 $[Au_2(SC_6H_{11})(PPh_3)_2]$
4	940 (M^+), 884, 856, 828, 800 (M^+ − nCO, n = 2–5), 744, 716, 688 (M^+ − nCO, n = 7–9), 660 $[Fe_3\{Au(PPh_3)\}(SH)]$, 659 $[Fe_3\{Au(PPh_3)\}S]$, 459 $[Au(PPh_3)]$, 721 $[Au(PPh_3)_2]$, 979 $[Au_2(SEt)(PPh_3)_2]$
5	882 (M^+), 798, 770, 742, 714, 686 (M^+ − nCO, n = 3–7), 604 $[Fe_2\{Au(PPh_3)\}(SH)]$, 603 $[Fe_2\{Au(PPh_3)\}S]$, 459 $[Au(PPh_3)]$, 721 $[Au(PPh_3)_2]$, 1033 $[Au_2(SC_6H_{11})(PPh_3)_2]$
6	828 (M^+), 800, 772, 744, 716, 688, 660, 632 (M^+ − nCO, n = 1–7), 604 $[Fe_2\{Au(PPh_3)\}(SH)]$, 603 $[Fe_2\{Au(PPh_3)\}S]$, 459 $[Au(PPh_3)]$, 721 $[Au(PPh_3)_2]$, 979 $[Au_2(SEt)(PPh_3)_2]$

The FAB mass spectra of the positive ions of **1–4** were recorded using 3-nitrobenzyl alcohol as the matrix (Table 2) and show the parent molecular ion in high abundance. These spectra are somewhat complex and can be explained in terms of a primary fragmentation involving stepwise loss of carbonyl groups from the parent ion to give $[Fe_3(SR)\{Au(PPh_3)\}]^+$, followed by elimination of an olefinic group to give $[Fe_3(SH)\{Au(PPh_3)\}]^+$ and finally loss of hydrogen to afford $[Fe_3S\{Au(PPh_3)\}]^+$. For complex **3**, degradation of the latter ion to $[Fe_3\{Au(PPh_3)\}]^+$ and Fe_3^+ has also been observed. An interesting feature of the spectra of **1–4** is the preferential loss of carbon monoxide to olefin, as compared with the easy rupture of the C–S bond in the series of $[Fe_3(CO)_9(\mu_3\text{-SR})(\mu\text{-H})]$ to give $[Fe_3(CO)_9(\mu_3\text{-S})]^-$ or $[Fe_3(CO)_9(\mu_3\text{-S})]^{2-}$ when heated in polar solvents, probably through a radical pathway.[14] It is interesting that the pattern shown in all these spectra is similar to that reported for the closely related $[Fe_3(CO)_9(\mu_3\text{-SR})$-

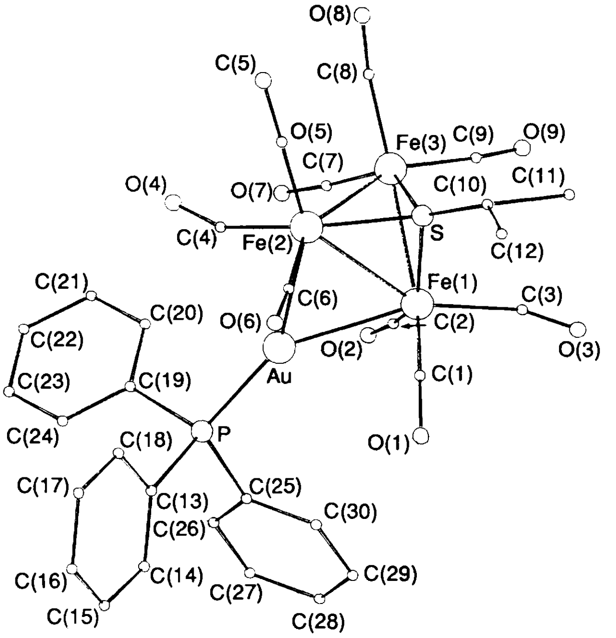

Fig. 1 Molecular structure of $[Fe_3(CO)_9(\mu_3\text{-}SPr^i)\{\mu\text{-}Au(PPh_3)\}]$ showing the atom labelling scheme

Table 3 Selected bond lengths (Å) and angles (°) for compound **1**

Fe(1)–Au	2.653(4)	Fe(2)–Au	2.645(5)
Fe(2)–Fe(1)	2.800(6)	Fe(3)–Fe(1)	2.631(8)
C(1)–Fe(1)	1.71(4)	C(2)–Fe(1)	1.70(5)
Fe(3)–Fe(2)	2.644(7)	S–Fe(2)	2.132(9)
C(5)–Fe(2)	1.79(6)	C(6)–Fe(2)	1.78(4)
C(7)–Fe(3)	1.80(4)	C(8)–Fe(3)	1.80(5)
C(10)–S	1.73(8)	C(1)–O(1)	1.26(4)
C(3)–O(3)	1.06(4)	C(4)–O(4)	1.12(4)
C(6)–O(6)	1.20(4)	C(7)–O(7)	1.17(4)
C(9)–O(9)	1.09(4)	S–Fe(3)	2.14(1)
P–Au	2.251(8)	C(9)–Fe(3)	1.87(5)
S–Fe(1)	2.109(10)	C(2)–O(2)	1.22(5)
C(3)–Fe(1)	2.04(4)	C(5)–O(5)	1.29(5)
C(4)–Fe(2)	1.83(4)	C(8)–O(8)	1.12(4)
Fe(2)–Au–Fe(1)	63.8(1)	P–Au–Fe(1)	143.1(2)
P–Au–Fe(2)	152.2(2)	Fe(2)–Fe(1)–Au	57.9(1)
Fe(3)–Fe(1)–Au	97.2(2)	Fe(3)–Fe(1)–Fe(2)	58.2(2)
S–Fe(1)–Au	106.4(3)	S–Fe(1)–Fe(2)	49.0(2)
S–Fe(1)–Fe(3)	52.1(4)	Fe(1)–Fe(2)–Au	58(1)
Fe(3)–Fe(2)–Au	97(2)	Fe(3)–Fe(2)–Fe(1)	58(2)
S–Fe(2)–Au	106(3)	S–Fe(2)–Fe(1)	48(3)
S–Fe(2)–Fe(3)	52(3)	Fe(2)–Fe(3)–Fe(1)	64.1(2)
S–Fe(3)–Fe(1)	51.2(3)	S–Fe(3)–Fe(2)	51.6(3)
Fe(2)–S–Fe(1)	82.7(3)	Fe(3)–S–Fe(1)	76.6(4)
Fe(3)–S–Fe(2)	76.6(4)		

$(\mu\text{-}H)]$[16] which shows that the formal substitution of a hydride by the $Au(PPh_3)$ fragment scarcely affects the fragmentation process.

The new complexes **5** and **6** were characterized spectroscopically and their parameters were almost identical to those reported for the recently described $[Fe_2(CO)_6(\mu\text{-}CO)(\mu\text{-}SR)\{\mu\text{-}Au(PPh_3)\}]$ clusters[10] (Table 1).

Attempts to obtain the analogous copper and silver derivatives were unsuccessful. Although the IR, ^1H and ^{31}P NMR parameters revealed that they are actually formed in thf solution, the high instability of these species precluded their isolation as solids. This is in good agreement with what is observed for other metal clusters involving Group 11 metals.[2]

Description of the Crystal Structure of $[Fe_3(CO)_9(\mu_3\text{-}SPr^i)\{\mu\text{-}Au(PPh_3)\}]$ **1**.—The structure of cluster **1** was determined by X-ray diffraction. A view of the molecule is shown in Fig. 1, together with the atomic numbering scheme; the most important bond distances and angles are given in Table 3. The structure may be regarded as derived from that of $[Fe_3(CO)_9(\mu_3\text{-}SPr^i)(\mu\text{-}H)]$[18] by replacing the hydride ligand by the gold atom from the $Au(PPh_3)$ ligand. Thus, the $Au(PPh_3)$ group bridges one edge of the Fe_3 triangle and the four metal atoms form a butterfly arrangement similar to those found in several related complexes. The resulting butterfly angle for this cluster is 123.9(2)°, which is between the values found in two independent molecules of $[Fe_3(CO)_9(\mu_3\text{-}HC{=}NBu^t)\{\mu\text{-}Au(PPh_3)\}]$ (110.9 and 132.1°),[9] but significantly less obtuse than that reported for $[Ru_3(CO)_9(\mu_3\text{-}SBu^t)\{\mu\text{-}Au(PPh_3)\}]$ (147.5°).[19] Although one report has attempted to relate the dihedral angles between the wings to the cluster electron count,[20] suggesting that the more electron-rich species may open out to become nearly flat, other studies indicate that packing forces may be responsible for the resulting dihedral angle.[9] The SPr^i ligand is bonded almost symmetrically to all three iron atoms; the Fe–S distances, 2.11(1), 2.13(1) and 2.14(1) Å, are notably shorter than those found in the two structurally investigated iron–gold thiolate-bridged complexes: $[Fe_2(CO)_6(\mu\text{-}CO)(\mu\text{-}SPr^i)\{\mu\text{-}Au(PPh_3)\}]$ [2.263(2), 2.270(2) Å][10] and $[Fe_2(CO)_6(\mu\text{-}CO)(\mu,\eta^2\text{-}SC_{11}H_{19})\{\mu\text{-}Au(PPh_3)\}]$ [2.213(7), 2.205(5) Å].[21] Comparison with the μ-hydrido complex $[Fe_3(CO)_9(\mu_3\text{-}SPr^i)(\mu\text{-}H)]$ shows that the presence of the $Au(PPh_3)$ group in **1** results in a lengthening of the Fe(1)–Fe(2) separation by 0.13 Å; this enlarging effect on replacing μ-H by the isolobal μ-$Au(PPh_3)$ has been observed previously.[22] On the other hand, the iron–gold distances [2.653(4), 2.645(5) Å] compare well with those reported for $[Fe_2(CO)_6(\mu\text{-}CO)(\mu\text{-}SPr^i)\{\mu\text{-}Au(PPh_3)\}]$ and $[Fe_2(CO)_6(\mu\text{-}CO)(\mu,\eta^2\text{-}SC_{11}H_{19})\{\mu\text{-}Au(PPh_3)\}]$ clusters (average of four iron–gold lengths = 2.680 Å) although they are longer than those found in terminal Au–Fe bonds in $[Fe_2Au_2(CO)_8(\mu\text{-}dppm)]$ [dppm = bis(diphenylphosphino)methane] [2.534(2) and 2.527(2) Å][3] and in $[AuFe\{Si(OMe)_3\}(CO)_3(\mu\text{-}dppm)]_2\cdot CH_2Cl_2$ [2.535(3) and 2.562(3) Å].[4] Finally, it is of interest to point out that the butterfly configuration is usually associated with a 62-electron count[23] and this number is not attained by **1** considering that the $Au(PPh_3)$ fragment produces an increment of 12 to the polyhedral electron count of the cluster, according to the condensation rules given by the polyhedral skeletal electron pair theory,[24] and that the $\mu_3\text{-}SPr^i$ functions as a five-electron donor.

Experimental

General.—All reactions were carried out under an atmosphere of pre-purified N_2 using Schlenk techniques. Solvents were dried by standard methods. Elemental analyses of C and H were carried out with a Perkin Elmer 2400 microanalyser O Proton, $^{31}P\text{-}\{^1H\}$ and $^{13}C\text{-}\{^1H\}$ NMR spectra were recorded on a Bruker AMX 300 or on a Varian Unity 300, IR (range 4000–200 cm^{-1}) spectra on a Nicolet 5 DX FT spectrophotometer. The FAB positive-ion mass spectra were recorded on a VG Autospec spectrometer. The complex $[Au(PPh_3)Cl]$[25] was prepared as described previously.

Synthesis of $Li[Fe_3(CO)_9(\mu\text{-}SR)]$ ($R = Pr^i$, Bu^t, C_6H_{11} *or* Et).—To a solution of LiBu (2.2 mmol) in thf (30 cm^3) at −78 °C was added with stirring the corresponding thiol, RSH (2.2 mmol). This solution was slowly allowed to reach 0 °C and was then added to a suspension of $[Fe_3(CO)_{12}]$ (2.2 mmol) in thf (10 cm^3) at 40 °C. The resulting solution, which became red immediately, was refluxed for 0.5 h. The solvent was evaporated *in vacuo*, and the viscous residue was extracted with hexane to remove $[\{Fe(CO)_3(SR)\}_2]$ derivatives formed as by-products.

Table 4 Final atomic coordinates ($\times 10^4$) for compound **1**

Atom	*X*/*a*	*Y*/*b*	*Z*/*c*
Au	22 376(6)	9 264(8)	2 394(4)
Fe(1)	2 655(2)	1 945(3)	1 655(2)
Fe(2)	3 207(2)	2 834(3)	525(1)
Fe(3)	4 132(2)	2 101(3)	1 933(2)
P	1 608(3)	−714(5)	−490(3)
S	3 925(4)	3 566(5)	1 637(3)
O(1)	1 015(12)	2 648(19)	891(10)
O(2)	2 881(11)	−763(18)	1 776(10)
O(3)	2 512(11)	2 076(17)	3 249(9)
O(4)	3 778(11)	936(20)	−249(10)
O(5)	4 396(13)	4 514(21)	209(12)
O(6)	1 791(11)	3 984(18)	−608(10)
O(7)	4 338(11)	−469(19)	1 402(10)
O(8)	5 500(12)	3 362(18)	1 920(10)
O(9)	4 640(14)	1 569(22)	3 630(12)
C(1)	1 728(16)	2 443(23)	1 210(12)
C(2)	2 775(16)	367(30)	1 771(12)
C(3)	2 720(22)	1 908(33)	2 790(16)
C(4)	3 414(15)	1 541(22)	−28(12)
C(5)	3 900(18)	3 811(28)	346(14)
C(6)	2 328(16)	3 457(23)	−137(13)
C(7)	4 239(14)	529(21)	1 622(12)
C(8)	4 996(16)	2 789(28)	1 906(16)
C(9)	4 421(18)	1 819(26)	3 008(16)
C(10)	3 150(31)	5 033(48)	1 961(20)
C(11)	3 356(19)	5 017(29)	2 898(17)
C(12)	2 563(36)	6 175(58)	1 636(33)
C(13)	817(8)	−364(15)	−1 401(6)
C(14)	96(8)	−931(15)	−1 649(6)
C(15)	−466(8)	−586(15)	−2 363(6)
C(16)	−307(8)	326(15)	−2 829(6)
C(17)	414(8)	892(15)	−2 580(6)
C(18)	976(8)	547(15)	−1 866(6)
C(19)	2 265(9)	−1 728(13)	−758(9)
C(20)	3 027(9)	−1 899(13)	−262(9)
C(21)	3 491(9)	−2 747(13)	−465(9)
C(22)	3 192(9)	−3 425(13)	−1 164(9)
C(23)	2 430(9)	−3 253(13)	−1 659(9)
C(24)	1 966(9)	−2 405(13)	−1 456(9)
C(25)	1 162(8)	−1 754(13)	17(8)
C(26)	1 162(8)	−3 058(13)	−63(8)
C(27)	818(8)	−3 814(13)	336(8)
C(28)	474(8)	−3 266(13)	815(8)
C(29)	474(8)	−1 962(13)	896(8)
C(30)	818(8)	−1 206(13)	497(8)

Preparation of Complexes $[Fe_3(CO)_9(\mu_3\text{-}SR)\{\mu\text{-}Au(PPh_3)\}]$ (R = Pr^i **1**, Bu^t **2**, C_6H_{11} **3** *or* Et **4**).—Details of the synthesis of **1** also apply to **2**–**4**. To a thf solution (40 cm^3) of $Li[Fe_3(CO)_9(\mu\text{-}SPr^i)]$ (0.8 g, 1.59 mmol) was added $[Au(PPh_3)Cl]$ (0.82 g, 1.59 mmol) and $TlBF_4$ (0.46 g, 1.59 mmol) at room temperature. The mixture was stirred and the solution became maroon. After being stirred for 1 h, the mixture was filtered through a pad of Celite and the solvent was eliminated *in vacuo*. The resulting residue was chromatographed on silica gel 100. Elution with hexane yielded traces of one orange band of $[\{Fe(CO)_3(\mu\text{-}SPr^i)\}_2]$. Elution with thf–hexane (1 : 3) gave traces of the green $[Fe_2(CO)_6(\mu\text{-}CO)(\mu\text{-}SPr^i)\{\mu\text{-}Au(PPh_3)\}]$ derivative and finally, elution with thf–hexane (1 : 1) afforded a red-purple band of $[Fe_3(CO)_9(\mu_3\text{-}SPr^i)\{\mu\text{-}Au(PPh_3)\}]$ (1.24 g, 82% yield).

For R = Bu^t, operating as above, the following compounds were isolated: elution with hexane, $[\{Fe(CO)_3(\mu\text{-}SBu^t)\}_2]$ (4%); with thf–hexane (1 : 1), $[Fe_3(CO)_9(\mu_3\text{-}SBu^t)\{\mu\text{-}Au(PPh_3)\}]$ (85%); with thf, traces of $Li[Fe_3(CO)_9(\mu\text{-}SBu^t)]$.

For R = C_6H_{11}, the following species were obtained: elution with hexane, $[\{Fe(CO)_3(\mu\text{-}SC_6H_{11})\}_2]$(traces); elution with thf–hexane (2 : 1), $[Fe_2(CO)_6(\mu\text{-}CO)(\mu\text{-}SC_6H_{11})\{\mu\text{-}Au(PPh_3)\}]$ (30%); with thf, $[Fe_3(CO)_9(\mu_3\text{-}SC_6H_{11})\{\mu\text{-}Au(PPh_3)\}]$ (57% yield) and traces of $Li[Fe_3(CO)_9(\mu\text{-}SC_6H_{11})]$ by elution with ethanol.

For R = Et, after elution with hexane, $[\{Fe(CO)_3(\mu\text{-}SEt)\}_2]$ (3%); with thf–hexane (1 : 10), the green complex $[Fe_2(CO)_6(\mu\text{-}CO)(\mu\text{-}SEt)\{\mu\text{-}Au(PPh_3)\}]$ (60%); with thf–hexane (1 : 5), $[Fe_3(CO)_9(\mu_3\text{-}SEt)\{\mu\text{-}Au(PPh_3)\}]$ (10% yield) and traces of $Li[Fe_3(CO)_9(\mu_3\text{-}SEt)]$ were detected by elution with thf.

Crystallography.—*Crystal data.* $C_{30}H_{22}AuFe_3O_9PS$ **1**, M = 954.05, monoclinic, space group $P2_1/c$, a = 18.745(3), b = 10.638(2), c = 18.345(3) Å, β = 111.57(3)°, U = 3402(2) Å^3, Z = 4, D_c = 1.862 g, cm^{-3}, $F(000)$ = 1848.0, λ(Mo-Kα) = 0.710 69 Å, μ(Mo-Kα) = 58.70 cm^{-1}.

Data collection. A prismatic crystal (0.1 × 0.1 × 0.2 mm) was selected and mounted on a Philips PW-1100 diffractometer. Unit-cell parameters were determined from automatic centring of 25 reflections ($12 \leqslant \theta \leqslant 18°$) and refined by least-squares methods. Intensities were collected with graphite-monochromatized Mo-Kα radiation, using ω–2θ scan technique. 4064 Reflections were measured in the range $2 \leqslant \theta \leqslant 30°$, 2256 of which were assumed as observed applying the condition $I \geqslant 2.5\sigma(I)$. Three reflections were measured every 2 h as orientation and intensity controls and significant intensity decay was not observed. Lorentz-polarization and absorption corrections were made.

Structure solution and refinement. The structure was solved by a Patterson synthesis, using the SHELXS computer program[26] and refined by the full-matrix least-squares method with the SHELX 76 computer program.[27] The function minimized was $\Sigma w(|F_o| - |F_c|)^2$, where $w = \sigma^{-2}(F_o)$; f, f', and f'' were taken from ref. 28. Phenyl rings were refined as 'rigid groups' with C–C 1.396 Å and C–C–C 120° and using an overall anisotropic coefficient for each phenyl ring. The final R factor was 0.044 (R' = 0.044) for all observed reflections. The number of refined parameters was 280. The maximum shift/estimated standard deviation was 0.1; maximum and minimum peaks in the final difference synthesis were 0.6 and −0.4 e Å^{-3}, respectively. Atomic coordinates are listed in Table 4.

Additional material available from the Cambridge Crystallographic Data Centre comprises thermal parameters and remaining bond distances and angles.

Acknowledgements

Financial support was generously provided by Dirección General de Investigacion Cientifica y Tecnica (Spain) (Project PB90-0055-C02-01).

References

1 D. A. Roberts and G. L. Geoffroy, in *Comprehensive Organometallic Chemistry*, eds. G. Wilkinson, F. G. A. Stone and E. W. Abel, Pergamon, Oxford, 1982.

2 I. D. Salter, *Adv. Organomet. Chem.*, 1989, **29**, 249.

3 S. Alvarez, O. Rossell, M. Seco, J. Valls, M. A. Pellinghelli and A. Tiripicchio, *Organometallics*, 1991, **10**, 2309.

4 P. Braunstein, M. Knorr, A. Tiripicchio and M. Tiripicchio Camellini, *Inorg. Chem.*, 1992, **31**, 3685.

5 K. Fischer, M. Muller and H. Vahrenkamp, *Angew. Chem., Int. Ed. Engl.*, 1984, **23**, 140.

6 M. Ferrer, R. Reina, O. Rossell, M. Seco and X. Solans, *J. Chem. Soc., Dalton Trans.*, 1991, 347.

7 R. Reina, O. Rossell, M. Seco, J. Ros, R. Yáñez and A. Perales, *Inorg. Chem.*, 1991, **30**, 3973.

8 C. P. Horwitz, E. M. Holt, C. P. Brock and D. F. Shriver, *J. Am. Chem. Soc.*, 1985, **107**, 8136.

9 M. I. Bruce and B. K. Nicholson, *J. Organomet. Chem.*, 1983, **250**, 627.

10 E. Delgado, E. Hernández, O. Rossell, M. Seco, E. Gutierrez Puebla and C. Ruíz, *J. Organomet. Chem.*, in the press.

11 J. A. de Beer and R. J. Haines, *Chem. Commun.*, 1970, 288.

12 J. W. Lauher and K. Wald, *J. Am. Chem. Soc.*, 1981, **103**, 7648.

13 E. Delgado and E. Hernández, *Polyhedron*, 1992, **11**, 3135.

14 J. Takács and L. Markó, *J. Organomet. Chem.*, 1983, **247**, 223.

15 A. Winter, L. Zsolnai and G. Huttner, *J. Organomet. Chem.*, 1983, **250**, 409.

16 J. A. de Beer and R. J. Haines, *J. Organomet. Chem.*, 1970, **24**, 757.

17 A. Winter, L. Zsolnai and G. Huttner, *Chem. Ber.*, 1982, **115**, 1286.

18 R. Bau, B. Don, R. Greatrex, R. J. Haines, R. A. Love and R. D. Wilson, *Inorg. Chem.*, 1975, **14**, 3021.

19 M. I. Bruce, O. B. Shawkataly and B. K. Nicholson, *J. Organomet. Chem.*, 1985, **286**, 427.

20 A. J. Carty, S. A. MacLaughlin, J. V. Wagner and N. J. Taylor, *Organometallics*, 1982, **1**, 1013.

21 H. Umland and U. Behrens, *J. Organomet. Chem.*, 1985, **287**, 109.

22 M. I. Bruce, E. Horn, J. G. Matisons and M. R. Snow, *J. Organomet. Chem.*, 1985, **286**, 271.

23 W. Lauher, *J. Am. Chem. Soc.*, 1978, **100**, 5305; *J. Organomet. Chem.*, 1981, **213**, 25.

24 See, for example, D. M. P. Mingos and A. S. May, in *The Chemistry of Metal Cluster Complexes*, eds. D. F. Shriver, H. D. Kaesz and R. D. Adams, VCH, New York, 1990.

25 C. Kowala and J. M. Swan, *Aust. J. Chem.*, 1966, **19**, 547.

26 G. M. Sheldrick, *Acta Crystallogr., Sect. A*, 1990, **46**, 467.

27 G. M. Sheldrick SHELX 76, a Program for Crystal Structure Determination, University of Cambridge, Cambridge, 1976.

28 *International Tables of X-Ray Crystallography*, Kynoch Press, Birmingham, 1974, vol. 4, pp. 99, 100, 149.

Received 18*th February* 1993; *Paper* 3/00977G